

Flavor-changing single top quark production channels at e^+e^- colliders in the effective Lagrangian description

S. Bar-Shalom* and J. Wudka†

Department of Physics, University of California, Riverside, California 92521

(Received 27 May 1999; published 8 October 1999)

We perform a global analysis of the sensitivity of CERN LEP2 and e^+e^- colliders with a c.m. energy in the range 500–2000 GeV to new flavor-changing single top quark production in the effective Lagrangian approach. The processes considered are sensitive to new flavor-changing effective vertices such as Ztc , htc , and four-Fermi $tcee$ contact term as well as a right-handed Wtb coupling. We show that e^+e^- colliders are most sensitive to the physics responsible for the contact $tcee$ vertices. For example, it is found that the recent data from the 189 GeV LEP2 run can be used to rule out any new flavor physics that can generate these four-Fermi operators up to energy scales of $\Lambda \gtrsim 0.7\text{--}1.4$ TeV, depending on the type of the four-Fermi interaction. We also show that a corresponding limit of $\Lambda \gtrsim 1.3\text{--}2.5$ and $\Lambda \gtrsim 17\text{--}27$ TeV can be reached at the future 200 GeV LEP2 run and a 1000 GeV e^+e^- collider, respectively. We note that these limits are much stronger than the typical limits which can be placed on flavor diagonal four-Fermi couplings. Similar results hold for $\mu^+\mu^-$ colliders and for $t\bar{u}$ associated production. Finally we briefly comment on the necessity of measuring *all* flavor-changing effective vertices as they can be produced by different types of heavy physics. [S0556-2821(99)01221-7]

PACS number(s): 13.85.Rm, 12.20.Fv, 13.90.+i, 14.65.Ha

I. INTRODUCTION

One of the fundamental unresolved issues in high-energy physics is the origin of the observed (quark) flavor structure. Within the standard model (SM) flavor-changing processes are controlled by the scalar sector, and are such that tree-level flavor-changing neutral currents (FCNC) are absent. This opens the possibility of using the corresponding flavor-changing processes to probe new physics whose effects may include appreciable violation of natural flavor conservation already at energies probed by present high energy colliders. For this reason, searching for new flavor-changing dynamics will be one of the major goals of the next generation of high energy colliders such as an e^+e^- Next Linear Collider (NLC) [1].

The top quark, which is the least tested fermion in the SM, can play an important role in our understanding of flavor dynamics since its large mass makes it more sensitive to certain types of flavor changing interactions. In particular, $t \rightarrow c$ (or $t \rightarrow u$) transitions which may lead to FCNC signals in high energy colliders, offer a unique place for testing the SM flavor structure. Below we note that, in addition to direct observations in top quark production and decays, the gauge structure of the SM can be used to constrain flavor-changing processes involving the top quark through existing data on B meson decays.

Top-charm flavor-changing processes can be studied either in $t \rightarrow c$ decays or in $t\bar{c}$ pair production in collider experiments. In the SM such decays [2,3] and production [4] processes are unobservably small since they occur at the one-loop level and in addition are Glashow-Iliopoulos-Maiani

(GIM) suppressed. Thus, any signal of such $t \rightarrow c$ transitions will be a clear evidence of new flavor physics beyond the SM. This fact has led to a lot of theoretical activity involving top-charm transitions within some specific popular models beyond the SM, for example, studies of $t \rightarrow c$ decays in multi Higgs doublets models (MHDM) [2,5–7], in supersymmetry with R -parity conservation [8] and with R -parity violation [9,10], and studies of $t\bar{c}$ production in MHDM [6,7,11], in supersymmetry with R -parity violation [10,12] and in models with extra vector-like quarks [13]. In this paper we will use instead a model independent approach [14] to investigate $t\bar{c}$ (and¹ $\bar{t}c$) pair production in e^+e^- colliders such as CERN LEP2 and a Next Linear Collider (NLC) with c.m. energies of 500–2000 GeV [1].

It is important to stress the advantage of studying $t\bar{c}$ production over $t \rightarrow c$ decays signals in high energy collider experiments in such a model independent approach. While $t \rightarrow c$ decays will be suppressed by powers of m_t/Λ , where Λ indicates the heavy physics energy scale, the corresponding suppression factor for $t\bar{c}$ production processes is proportional to a power of E_{CM}/Λ , where E_{CM} is the c.m. energy of the collider. From the experimental point of view, a $t\bar{c}$ signal has some very distinct characteristics, in particular, it has the unique signature of producing a single b -jet in the final state. In a recent paper [15] we have observed that the SM cross sections for processes with an odd number of b -jets in the final state are extremely small, which allows the definition of a new approximately conserved quantum number:

¹Throughout this paper we will loosely refer to a $t\bar{c} + \bar{t}c$ final state by $t\bar{c}$. The contributions from the charged conjugate $\bar{t}c$ state are included in our numerical results unless explicitly stated otherwise.

*Email address: shaouly@phyun0.ucr.edu

†Email address: jose.wudka@ucr.edu

b -parity (b_p). Processes with even or odd number of b jets have $b_p=1$ and $b_p=-1$ respectively. Thus the b_p -odd process $e^+e^- \rightarrow t\bar{c}$ can be detected using the simple b -jet counting method suggested in [15], and is essentially free of any SM irreducible background.²

Several model-independent studies of $t\bar{c}$ pair production have appeared in the literature, where the signatures and observability of these flavor violating processes were investigated in e^+e^- colliders [13,16–18], hadronic colliders [19] and $\gamma\gamma$ colliders [20]. The present paper extends the results obtained in [16–18] by performing a model-independent analysis in a wider variety of channels. In particular, we explore the sensitivity of e^+e^- colliders to all relevant effective operators that can give rise to $t\bar{c}$ production in e^+e^- colliders with a c.m. energy ranging from³ 189 GeV (LEP2) to 2000 GeV. We consider the $2 \rightarrow 2$ processes $e^+e^- \rightarrow t\bar{c}$, $e^+e^- \rightarrow Zh$ followed by $h \rightarrow t\bar{c}$, where h is the SM Higgs-boson, and the t -channel fusion processes W^+W^- , $ZZ \rightarrow t\bar{c}$. These reactions can proceed via new Ztc , htc and Wtb couplings as well as through new $tcee$ four-Fermi effective operators that have not been previously considered in this context.

We argue that since the effective interactions are but the low energy manifestations of an underlying theory, and assuming this heavy theory is a gauge theory containing fermions, scalars and gauge-bosons, some of the effective vertices that contribute to $e^+e^- \rightarrow t\bar{c}$ are expected to be suppressed and will produce very small effects (the Ztc and γtc magnetic-type couplings considered in [17,18] fall into this category). We therefore do not include such couplings (see Sec. II). We will concentrate on those vertices for which general principles do not mandate a small coefficient.

Following the above viewpoint, our study indicates that the reaction $e^+e^- \rightarrow t\bar{c}$ is most sensitive to effective four-Fermi flavor-changing interactions. It is found, for example, that if the coupling strength of the four-Fermi interactions is of $\mathcal{O}(1/\Lambda^2)$ as expected by naturalness, then tens to hundreds $t\bar{c}$ events should show up already at LEP2 energies when $\Lambda \lesssim 1$ TeV. Alternatively, if no $e^+e^- \rightarrow t\bar{c}$ signal is observed, then the limits that can be placed on the energy scale Λ of such four-Fermi effective operators are quite strong; the data accumulated at the recent 189 GeV LEP2 run can already place the limit $\Lambda \gtrsim 0.7-1.4$ TeV, while $\Lambda \gtrsim 1.5-2.5$ TeV will be achievable at a 200 GeV LEP2 and reaches $\Lambda \gtrsim 17-27$ TeV at a NLC with a c.m. energy of 1000 GeV (depending on the type of the four-Fermi operator). It is remarkable that a 500–1000 GeV e^+e^- collider can place a bound on such four-Fermi dynamics which is almost 20–30 times larger than its c.m. energy. These limits can be compared, for example, with the bound $\Lambda \gtrsim 5$ TeV

that can be obtained on $eeee$ and $ttee$ four-Fermi operators by studying the reactions $e^+e^- \rightarrow e^+e^-$ [21] and $e^+e^- \rightarrow t\bar{t}$ [22] at a NLC. Note, however, that the scales responsible for the $tcee$ and $ttee$ (or $eeee$) vertices need not be the same. Similarly the effective $tcee$ and Ztc vertices may be produced by different physics, e.g., a heavy neutral vector boson (for $tcee$) vs. heavy vector-like quarks (for Ztc) [13]; there are new physics possibilities which are best probed through Ztc interactions. In all cases the sensitivity to Λ will be significantly degraded if the couplings are $\ll 1$.

Flavor violating Z and Higgs (h) interactions, such as possible effective Ztc and htc vertices, are probed via WW -fusion processes $e^+e^- \rightarrow W^+W^- \nu_e \bar{\nu}_e \rightarrow t\bar{c} \nu_e \bar{\nu}_e$, and the Bjorken process $e^+e^- \rightarrow Zh$ followed by $h \rightarrow t\bar{c}$ for htc . For example, if no $t\bar{c} \nu_e \bar{\nu}_e$ signal is observed at 1500 GeV (500 GeV) NLC, then $\Lambda \gtrsim 2$ TeV ($\gtrsim 800$ GeV), for a SM Higgs mass of 250 GeV, and assuming that the htc vertices have a coupling strength of $\mathcal{O}(v^2/\Lambda^2)$ (v is the vacuum expectation value of the SM scalar field). The effects of new Ztc and htc effective couplings on the ZZ -fusion process $e^+e^- \rightarrow ZZ e^+e^- \rightarrow t\bar{c} e^+e^-$ are too small to be detected at a NLC. The same is true of a right-handed Wtb coupling in the reaction $e^+e^- \rightarrow W^+W^- \nu_e \bar{\nu}_e \rightarrow t\bar{c} \nu_e \bar{\nu}_e$, even when assuming a coupling with a strength of $\mathcal{O}(v^2/\Lambda^2)$, the bound allowed by naturality.

We note that, since charm quark mass effects are negligible at high energy e^+e^- colliders, our results equivalently apply to $t\bar{u}$ pair production, in particular, to effective operators generating the corresponding tu flavor-changing interactions.

The paper is organized as follows: in Sec. II we describe the effective Lagrangian framework and extract the Feynman rules for the new effective vertices. In Sec. III we discuss the effects of new Ztc vector couplings and $tcee$ four-Fermi interactions in $e^+e^- \rightarrow t\bar{c}$ and W^+W^- , $ZZ \rightarrow t\bar{c}$. In Sec. IV we consider the contribution of new htc scalar couplings to $e^+e^- \rightarrow Zh \rightarrow Zt\bar{c}$ and to $W^+W^- \rightarrow t\bar{c}$. In Sec. V we investigate the effects of a new right-handed Wtb coupling on the process $W^+W^- \rightarrow t\bar{c}$ and in Sec. VI we summarize our results.

II. THE EFFECTIVE LAGRANGIAN DESCRIPTION AND $T\bar{c}$ PRODUCTION AT e^+e^- COLLIDERS

There are two different theoretical paths one can adopt to investigate physics beyond the SM. In the first, one uses a specific model to calculate such effects. The second is to follow a model-independent approach where the effects of any given high energy model are parametrized by the coefficients of a series of effective operators without reference to any specific underlying theory. The power of the model-independent approach lies in its generality, its potential deficiency is the large number of constants which might *a priori* contribute to any given reaction. In this paper we follow the second route.

Our basic assumption will be that there is a gauge theory underlying the SM, whose scale Λ is well separated from the

²There is, of course, a reducible background due to reduced b -tagging efficiency; see [15].

³To be specific we consider reactions in e^+e^- colliders, but the analysis performed is clearly extendable to muon colliders.

Fermi scale. Under these circumstances the low energy limit of the theory will consist of the SM Lagrangian plus corrections represented by a series of effective operators \mathcal{O}_i constructed using the SM fields and whose coefficients are suppressed by powers of $1/\Lambda$

$$\mathcal{L}_{eff} = \mathcal{L}_{SM} + \sum_{n=5}^{\infty} \frac{1}{\Lambda^{n-4}} \sum_i \alpha_i \mathcal{O}_i^n, \quad (1)$$

where each \mathcal{O} respects the gauge symmetries of the SM but not necessarily its global symmetries.⁴ The dominating effects are usually generated by the lowest-dimensional operators contributing to the process of interest (there are, however, some exceptions, see [14]). For the flavor-violating processes considered here the only relevant operators are those of dimension 6; if these are absent there will be no observable signal.

In the following discussion we will assume, for definiteness, that the theory underlying the SM is weakly coupled; but we expect our results to hold in general. The reason is that both in weakly and strongly coupled (natural) theories, the dominating flavor-changing effects (at least for the processes considered) are produced by the four-Fermi contact interactions, for which naturality allows the largest coefficients [23].

Now, it is important to note that general considerations require certain bounds for the coefficients α_i in Eq. (1). For weakly coupled underlying theories the key point is that the effective operators may correspond to either tree-level or loop exchanges of the heavy fields. Loop-generated interactions are suppressed by factors of $\sim 1/16\pi^2$ (and by powers of the coupling constants) compared to the tree-level induced operators. One therefore expects the effects of the high energy theory to manifest themselves predominantly through tree-level generated (TLG) operators. In what follows we consider only TLG operators and neglect those generated by loops involving the heavy particles.

The observables studied in this paper cannot distinguish between models with large values of Λ having tree-level flavor-changing interactions and those models with lower values of Λ for which flavor-changing processes occur only via loops. But this ambiguity is only academic when discussing heavy physics virtual effects, as neither of these situations will produce measurable effects. Only models whose scales lie below ~ 10 TeV and which generate flavor violation at tree-level will be observed through the processes considered in this paper.

We stress that this approach is in general different from the one adopted in many previous investigations which use the effective Lagrangian description to study new physics in present and future colliders. For example, we do not include anomalous dipole-like operators of the form ($V = \gamma$ or Z)

⁴For example operators of dimension 5, if present, necessarily violate lepton number, [14].

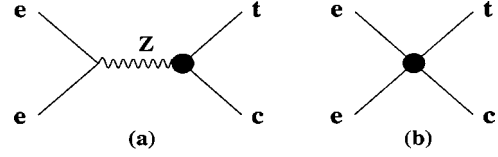


FIG. 1. Feynman diagrams that give rise to $e^+e^- \rightarrow t\bar{c}$ in the presence of (a) a new Ztc coupling and (b) a new $tcee$ four-Fermi coupling. The new effective vertex is denoted by a heavy dot.

$$ie\bar{t} \frac{\sigma_{\mu\nu} q^\nu}{m_t} (\kappa_V - i\tilde{\kappa}_V \gamma_5) c V^\mu, \quad (2)$$

in the reaction $e^+e^- \rightarrow t\bar{c}$, since the coefficients from these vertices are much smaller than those of the $tcee$ four-Fermi vertices. In fact, assuming the physics underlying the SM is weakly coupled, the typical sizes of the coefficients are $\kappa_V, \tilde{\kappa}_V \sim (v^2/\Lambda^2) \times 1/16\pi^2 \sim 4 \times 10^{-4}$, for $\Lambda \sim 1$ TeV. Thus the corresponding contributions are subdominant despite their rapid growth with energy. If instead κ_V or $\tilde{\kappa}_V \sim \mathcal{O}(1)$ [$\sim \mathcal{O}(0.1)$] is used—as required in order to have an appreciable $t\bar{c}$ production rate—what in fact is being done is to assume that the scale of “new physics” is $\Lambda \sim v/4\pi \sim 20$ GeV [$\Lambda \sim v/4 \sim 60$ GeV], which is of course unacceptable bearing the existing experimental evidence of the validity of the SM at these energy scales. Another loop induced effective operator that can give rise to a $t\bar{c}$ final state and that falls into this category is a $VVtc$ ($V=W$ or Z) contact term. In the following we will neglect these and similar contributions.

In contrast, new vector and pseudo-vector couplings in the Ztc vertex [note that the corresponding γtc couplings are forbidden by $U(1)$ gauge invariance] as well as new four-Fermi $tcee$ interactions, can arise from TLG effective operators and their coefficients can, therefore, take values typically of the order of $\sim (v^2/\Lambda^2)$. If present, these operators will give the dominant contribution to $t\bar{c}$ production; if these interactions are either absent or suppressed at tree-level, the $t\bar{c}$ production rate will be unobservably small. In the following we will investigate the possible effects due to TLG operators assuming no additional suppression factors are present.

We first list all the TLG effective operators contributing to $t\bar{c}$ pair production in high energy e^+e^- colliders via the processes

$$e^+e^- \rightarrow t\bar{c}, \quad (3)$$

$$e^+e^- \rightarrow Zh \rightarrow Zt\bar{c}, \quad (4)$$

$$e^+e^- \rightarrow W^+W^- \nu_e \bar{\nu}_e \rightarrow t\bar{c} \nu_e \bar{\nu}_e, \quad (5)$$

$$e^+e^- \rightarrow ZZ e^+e^- \rightarrow t\bar{c} e^+e^-. \quad (6)$$

Reaction (3) receives contributions from both an effective Ztc interaction [see Fig. 1(a)] and from four-Fermi $tcee$

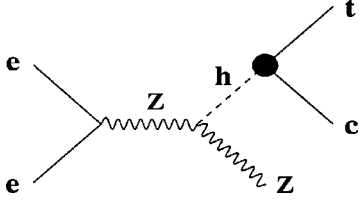


FIG. 2. Feynman diagram that gives rise to $e^+e^- \rightarrow Zt\bar{c}$ via the Bjorken process $e^+e^- \rightarrow Zh$ followed by $h \rightarrow t\bar{c}$, in the presence of a new htc coupling. The new effective vertex is denoted by a heavy dot.

effective operators [see Fig. 1(b)]. In reaction (4) we assume real Higgs boson (h) production followed by the Higgs boson decay $h \rightarrow t\bar{c}$, which occurs only in the presence of a new htc interaction as depicted in Fig. 2. Reaction (5) gets contributions from non-standard Ztc , htc and Wtd (d stands for any of the three down quarks in the SM) vertices as depicted in Figs. 3(a), 3(b) and 3(c), respectively. Finally, reaction (6) may receive contributions from non-standard htc as well as Ztc vertices as shown in Fig. 3(b) and Figs. 4(a) and 4(b). Below we list the TLG effective operators which give rise to such new couplings.

Our notation is the following [14]: q and l denote left-handed $SU(2)$ quark and lepton doublets, respectively; d , u and e for right-handed [$SU(2)$ singlet] down-quark, up-quark and charged lepton, respectively. The SM scalar doublet is denoted by ϕ and D is the covariant derivative. The Pauli matrices are denoted by τ_I , $I=1,2,3$. Also, although we suppress generation indices in the effective operators be-

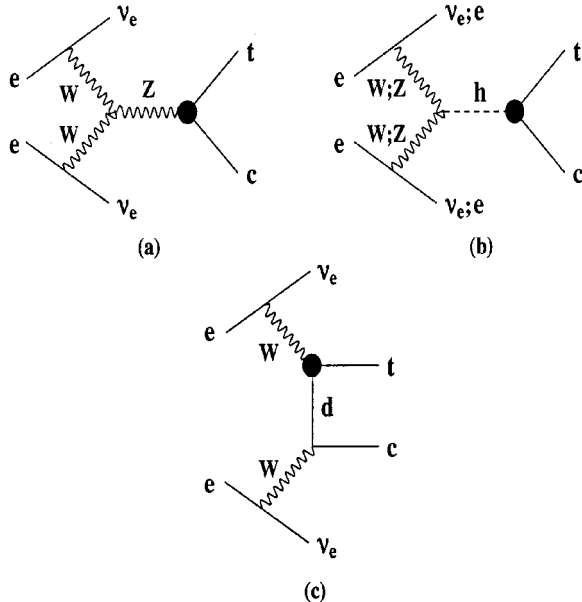


FIG. 3. Feynman diagrams that give rise to the WW -fusion process $e^+e^- \rightarrow t\bar{c}\nu_e\bar{\nu}_e$, in the presence of (a) a new Ztc coupling, (b) a new htc coupling and (c) a new Wtd coupling where $d=d, s$ or a b -quark. Also plotted in (b) is the Feynman diagram that gives rise to the ZZ -fusion process $e^+e^- \rightarrow t\bar{c}e^+e^-$ in the presence of a new htc coupling. The new effective vertex is denoted by a heavy dot.

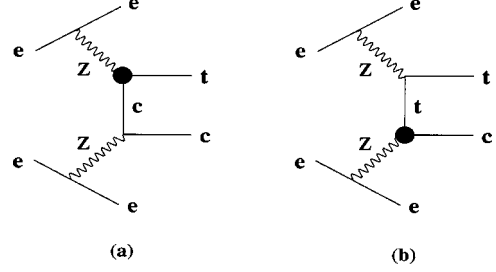


FIG. 4. Feynman diagrams that give rise to the ZZ -fusion process $e^+e^- \rightarrow t\bar{c}e^+e^-$ in the presence of a new Ztc coupling. The new effective vertex is denoted by a heavy dot.

low, it should be understood that the quark fields can correspond to different flavors in general, i.e., in our case \bar{q} or \bar{u} is the outgoing top quark and q or u is the incoming charm quark (or outgoing anti-charm quark).

A. Effective operators generating a Ztc vertex

There are three tree-level dimension 6 effective operators that can generate a new Ztc interaction. These are⁵ [14]

$$\begin{aligned} \mathcal{O}_{\phi q}^{(1)} &= i(\phi^\dagger D_\mu \phi)(\bar{q}\gamma^\mu q), \\ \mathcal{O}_{\phi q}^{(3)} &= i(\phi^\dagger D_\mu \tau^I \phi)(\bar{q}\gamma^\mu \tau^I q), \\ \mathcal{O}_{\phi u} &= i(\phi^\dagger D_\mu \phi)(\bar{u}\gamma^\mu u). \end{aligned} \quad (7)$$

Writing the new Ztc effective Lagrangian as

$$\mathcal{L}_{Z\mu tc} = g \frac{v^2}{\Lambda^2} \bar{t} \gamma_\mu (a_L^Z L + a_R^Z R) c, \quad (8)$$

where $L(R) = [1 - (+)\gamma_5]/2$, we can express the left and right couplings, a_L^Z and a_R^Z , in terms of the corresponding coefficients $\alpha_{\phi q}^{(1)}$, $\alpha_{\phi q}^{(3)}$ and $\alpha_{\phi u}$ [following our notation in Eq. (1)],

$$a_L^Z = \frac{1}{4c_W} (\alpha_{\phi q}^{(1)} - \alpha_{\phi q}^{(3)}), \quad a_R^Z = \frac{1}{4c_W} \alpha_{\phi u}, \quad (9)$$

where $c_W = \cos \theta_W$ and θ_W is the weak mixing angle.

The operators in Eq. (7) can be generated at tree-level by heavy gauge-boson or fermion exchange.

B. Effective operators generating a new htc vertex

Apart from the operators in Eqs. (7), which give rise also to a new htc interaction, there is an additional operator [14],

⁵Although we do not explicitly include the Hermitian conjugate operators, it should be clear that in our case, i.e., $t\bar{c}$ production, the effective operators for $\bar{t}c$ are the Hermitian conjugates of those that are given below for the $t\bar{c}$ final state.

$$\mathcal{O}_{u\phi} = (\phi^\dagger \phi)(\bar{q}u\tilde{\phi}). \quad (10)$$

Writing the new htc interaction Lagrangian as

$$\mathcal{L}_{htc} = g \frac{v^2}{\Lambda^2} \bar{t}(a_L^h L + a_R^h R)c, \quad (11)$$

we have (neglecting terms proportional to the charm quark mass)

$$a_L^h = \frac{m_t}{2gV}(\alpha_{\phi q}^{(1)} - \alpha_{\phi q}^{(3)}), \quad a_R^h = \frac{m_t}{2gV} \left(\alpha_{\phi u} + \frac{3v}{\sqrt{2}m_t} \alpha_{u\phi} \right). \quad (12)$$

The heavy excitations which can generate $\mathcal{O}_{u\phi}$ at tree-level are either heavy scalars mixing with the ϕ , and/or heavy fermions mixing with the light fermions and ϕ . In the first case there is a contribution only if the mixing occurs through $\mathcal{O}(\Lambda)$ cubic couplings and is suppressed in natural theories.

C. Effective operators that generate new Wtd_i and Wcd_i vertices

Here there are two operators. One is $\mathcal{O}_{\phi q}^{(3)}$ in Eq. (7), the second is

$$\mathcal{O}_{\phi\phi} = (\phi^\dagger \epsilon D_\mu \phi)(\bar{u}\gamma^\mu d), \quad (13)$$

with $\epsilon_{12} = -\epsilon_{21} = 1$.

We will parameterize the $Wt\bar{d}_i$ and $W\bar{c}d_i$ ($d_i = d, s$ or b for $i = 1, 2$ or 3 , respectively) vertices according to

$$\mathcal{L}_{W_\mu t\bar{d}_i} = \frac{v^2}{\Lambda^2} \frac{g}{\sqrt{2}} \bar{t} \gamma_\mu (V_{3i} L + \delta_{L,i}^s L + \delta_{R,i}^s R) d_i, \quad (14)$$

$$\mathcal{L}_{W_\mu \bar{c}d_i} = \frac{v^2}{\Lambda^2} \frac{g}{\sqrt{2}} \bar{d}_i \gamma_\mu (V_{2i}^* L + \delta_{L,i}^c L + \delta_{R,i}^c R) c, \quad (15)$$

where V is the Cabibbo-Kobayashi-Maskawa (CKM) matrix. Thus, if all the relevant coefficients are real (as assumed in this paper), then one has

$$\delta_{L,i}^s = \alpha_{\phi q}^{(3)} \Big|_i^t, \quad \delta_{R,i}^s = -\frac{1}{2} \alpha_{\phi\phi} \Big|_i^t, \quad (16)$$

$$\delta_{L,i}^c = \alpha_{\phi q}^{(3)} \Big|_i^c, \quad \delta_{R,i}^c = -\frac{1}{2} \alpha_{\phi\phi} \Big|_i^c.$$

Notice that, since the operators $\mathcal{O}_{\phi\phi}$ and $\mathcal{O}_{\phi q}^{(3)}$ may have different coefficients for different flavors (families) of the up and down quarks, in order to be as general as possible we have added the subscript i and the superscript t or c appropriately.

The heavy excitations that can generate $\mathcal{O}_{\phi\phi}$ are either a heavy gauge boson which couples to ϕ , or a heavy fermion which couples to the light fermions and to ϕ .

D. Four-Fermi effective operators producing a $tcee$ contact interaction

There are seven relevant four-Fermi operators that contribute to $e^+e^- \rightarrow t\bar{c}$:

$$\mathcal{O}_{lq}^{(1)} = \frac{1}{2} (\bar{l} \gamma_\mu l)(\bar{q} \gamma^\mu q), \quad (17)$$

$$\mathcal{O}_{lq}^{(3)} = \frac{1}{2} (\bar{l} \gamma_\mu \tau^l l)(\bar{q} \gamma^\mu \tau^l q), \quad (18)$$

$$\mathcal{O}_{eu} = \frac{1}{2} (\bar{e} \gamma_\mu e)(\bar{u} \gamma^\mu u), \quad (19)$$

$$\mathcal{O}_{lq} = (\bar{l} e) \epsilon(\bar{q} u), \quad (20)$$

$$\mathcal{O}_{qe} = (\bar{q} e) (\bar{e} q), \quad (21)$$

$$\mathcal{O}_{lu} = (\bar{l} u) (\bar{u} l), \quad (22)$$

$$\mathcal{O}_{lq'} = (\bar{l} u) \epsilon(\bar{q} e). \quad (23)$$

One can also parameterize the most general four-Fermi effective Lagrangian for the $t\bar{c}e^+e^-$ interaction in the form

$$\begin{aligned} \mathcal{L}_{tcee} = & \frac{1}{\Lambda^2} \sum_{i,j=L,R} [V_{ij} (\bar{e} \gamma_\mu P_i e)(\bar{t} \gamma^\mu P_j c) + S_{ij} (\bar{e} P_i e) \\ & \times (\bar{t} P_j c) + T_{ij} (\bar{e} \sigma_{\mu\nu} P_i e)(\bar{t} \sigma^{\mu\nu} P_j c)], \end{aligned} \quad (24)$$

where $P_{L,R} = (1 \mp \gamma_5)/2$, and express these vector-like (V_{ij}), scalar-like (S_{ij}) and tensor-like (T_{ij}) couplings in terms of the coefficients of the seven four-Fermi operators in Eqs. (17)–(23). We get (Fierz-transforming the last four operators)

$$\begin{aligned} V_{LL} &= \frac{1}{2} (\alpha_{lq}^{(1)} - \alpha_{lq}^{(3)}), & V_{LR} &= -\frac{1}{2} \alpha_{lu}, & V_{RR} &= \frac{1}{2} \alpha_{eu}, \\ V_{RL} &= -\frac{1}{2} \alpha_{qe}, \\ S_{RR} &= -\alpha_{lq} + \frac{1}{2} \alpha_{lq'}, & S_{LL} &= S_{LR} = S_{RL} = 0, \\ T_{RR} &= \frac{1}{8} \alpha_{lq'}, & T_{LL} &= T_{LR} = T_{RL} = 0. \end{aligned} \quad (25)$$

The four-Fermi operators can be generated through the exchange of heavy vectors and scalars. Note however that the list provided does not include tensor operators, which have been eliminated using Fierz transformations. It is therefore possible for a tensor exchange to be hidden in a series of operators involving scalars (and vice-versa). It is noteworthy that no LL tensor or LL , LR and RL scalar terms are generated by dimension 6 operators [they can be generated by dimension 8 operators and have coefficients $\sim (v/\Lambda)^4$].

III. tce FOUR-FERMI INTERACTIONS AND $e^+e^- \rightarrow t\bar{c}$

As discussed in the previous section, there are seven possible TLG four-Fermi effective operators [see Eqs. (17)–(23)] respecting the SM symmetries. The effects of such four-Fermi operators have not been investigated in $e^+e^- \rightarrow t\bar{c}$; in this section we calculate the contribution of these operators to this process.

Using the effective four-Fermi Lagrangian piece in Eq. (24), we obtain the amplitude for $e^+e^- \rightarrow t\bar{c}$

$$\mathcal{M}_{tce} = \frac{1}{\Lambda^2} \sum_{ij} \{V_{ij}(\bar{v}_e \gamma_\mu P_i u_e)(\bar{u}_t \gamma^\mu P_j v_c) + S_{ij}(\bar{v}_e P_i u_e) \times (\bar{u}_t P_j v_c) + T_{ij}(\bar{v}_e \sigma_{\mu\nu} P_i u_e)(\bar{u}_t \sigma_{\mu\nu} P_j v_c)\}, \quad (26)$$

where $i, j = L$ or R . Recall that the only non-zero scalar and vector couplings are S_{RR} and T_{RR} .

The cross sections for polarized incoming electrons and outgoing top quarks (i.e., left or right-handed electron and top quark) are then readily calculated (recall that we assume all the new couplings to be real)

$$\sigma_{e_L t_L} = \sigma(e_L^- e^+ \rightarrow t_L \bar{c}) = \mathcal{C} [2(1 + \beta_t) V_{LL}^2 + (1 - \beta_t) V_{LR}^2], \quad (27)$$

$$\sigma_{e_L t_R} = \sigma(e_L^- e^+ \rightarrow t_R \bar{c}) = \mathcal{C} [(1 - \beta_t) V_{LL}^2 + 2(1 + \beta_t) V_{LR}^2], \quad (28)$$

$$\sigma_{e_R t_L} = \sigma(e_R^- e^+ \rightarrow t_L \bar{c}) = \mathcal{C} \left[2(1 + \beta_t) V_{RL}^2 + (1 - \beta_t) V_{RR}^2 + \frac{1}{2}(1 + \beta_t)(3S_{RR}^2 + 16T_{RR}^2) \right], \quad (29)$$

$$\sigma_{e_R t_R} = \sigma(e_R^- e^+ \rightarrow t_R \bar{c}) = \mathcal{C} [(1 - \beta_t) V_{RL}^2 + 2(1 + \beta_t) V_{RR}^2 + 16(1 - \beta_t) T_{RR}^2], \quad (30)$$

where

$$\mathcal{C} = \frac{s}{\Lambda^4} \frac{\beta_t^2}{4\pi(1 + \beta_t)^3}, \quad (31)$$

and $\beta_t = (s - m_t^2)/(s + m_t^2)$. The total unpolarized cross section for production of $t\bar{c} + \bar{t}c$ pairs is then

$$\sigma_{tc} = \sigma(e^- e^+ \rightarrow t\bar{c} + \bar{t}c) = \sum_{i,j=L,R} \sigma_{e_i t_j}. \quad (32)$$

Notice that, by assumption, such four-Fermi interactions are induced by exchanges of a heavy field in the underlying high energy theory for which one is replacing the heavy particle propagator by $1/\Lambda^2$. Therefore, σ_{tc} is proportional to s/Λ^4 [see Eq. (31)] and grows with the c.m. energy for a fixed Λ . Clearly, for this approximation to be valid, Λ must be larger than \sqrt{s} .

A few more useful observations can be made already by looking at the polarized cross sections in Eqs. (27)–(30) above:

There are no interference effects between the different four-Fermi couplings V_{ij} , S_{RR} and T_{RR} ; the total cross section depends only on the square value of these couplings and is, therefore, maximal when all these couplings are non-zero.

The vector couplings appear in the total cross section only in the combination $\Sigma |V_{ij}|^2$.

Initial and/or final polarization of the incoming electrons and/or top quarks can distinguish between different sets of couplings, e.g., if the incoming electron beam is left polarized then only V_{LL} and V_{LR} can contribute to $t\bar{c}$ production.

Before continuing we note that the new Ztc couplings a_L^Z and a_R^Z in Eq. (8) also contribute to $e^+e^- \rightarrow t\bar{c}$ by interfering with the four-Fermi vector couplings V_{ij} . These effects can be included by redefining

$$V_{ij} \rightarrow V_{ij} + 4c_i^Z a_j^Z \frac{m_W m_Z}{s - m_Z^2}, \quad (33)$$

where $i, j = L, R$, and $c_L^Z = -1/2 + s_W^2$, $c_R^Z = s_W^2$ are the couplings of a Z-boson to a left or a right handed electron, respectively. The effects of such new Ztc vector couplings on $e^+e^- \rightarrow t\bar{c}$ were also recently investigated by Han and Hewett [17], who have made a detailed analysis of the sensitivity of 200–1000 GeV e^+e^- colliders to such new couplings. Here, for the process $e^+e^- \rightarrow t\bar{c}$, we instead focus mainly on the effects of the four-Fermi couplings which, as will be shown below, give the dominant contribution to σ_{tc} .

In Fig. 5 we plot the total cross section σ_{tc} (in fb) as a function of the c.m. energy of the e^+e^- collider, taking $\Lambda = 1$ TeV, and for different types of four-Fermi couplings; as expected, the four-Fermi effective couplings give contributions to σ_{tc} which grow with the c.m. energy. Due to this effect, the cross section can be rather large, ranging from about 30 fb to 300 fb and yielding tens to hundreds $t\bar{c}$ events (depending on the type of four-Fermi coupling) already at LEP2 energies. At a 1 TeV NLC we find that $\sigma_{tc} \sim 10^4 - 10^5$ fb if $\Lambda = 1$ TeV. Recall that σ_{tc} scales as $1/\Lambda^4$, therefore, even with $\Lambda \sim 10 - 20$ TeV σ_{tc} is of $\mathcal{O}(\text{fb})$ at a 1 TeV NLC.

For completeness we also plot σ_{tc} for non-zero Ztc couplings $a_L^Z = 1$ or $a_R^Z = 1$ (dashed line). Clearly, the effects of

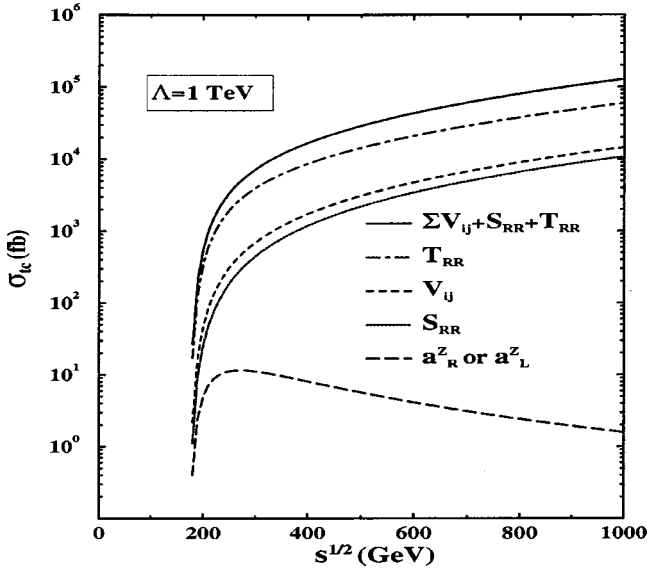


FIG. 5. The cross section $\sigma_{ic} = \sigma(e^+e^- \rightarrow t\bar{c} + t\bar{c})$ (in fb) is plotted as a function of the c.m. energy (\sqrt{s}) of the e^+e^- collider. The following cases are shown: all four-Fermi couplings are non-zero and equal 1, i.e., $V_{LL}=V_{LR}=V_{RL}=V_{RR}=S_{RR}=T_{RR}=1$ (solid line), only $T_{RR}=1$ (dot-dashed line), only one of the vector couplings V_{ij} equals 1 (dashed line), only $S_{RR}=1$ (dotted line) and either $a_L^Z=1$ or $a_R^Z=1$ with the four-Fermi couplings set to zero (long-dashed line). $\Lambda=1$ TeV is used for all cases.

such couplings are much smaller than those generated by the four-Fermi interactions. Even at LEP2 the contribution is about one to two orders of magnitudes smaller than the typical contribution from the four-Fermi interactions.

Notice also that, contrary to the four-Fermi case, the Ztc contributions to σ_{ic} drop as $\sim 1/s$ due to the explicit s -channel Z -boson propagator. Because of this, at a NLC with c.m. energies of $\sqrt{s} \gtrsim 1.5$ TeV, t -channel vector-boson fusion processes $W^+W^- \rightarrow t\bar{c}$ [see Fig. 3(a)] and $ZZ \rightarrow t\bar{c}$ [see Figs. 4(a) and 4(b)] become important and may be better probes of such Ztc couplings. We have calculated the total cross sections $\sigma_{WW} = \sigma(e^+e^- \rightarrow W^+W^- \nu_e \bar{\nu}_e \rightarrow t\bar{c} \nu_e \bar{\nu}_e)$ and $\sigma_{ZZ} = \sigma(e^+e^- \rightarrow ZZ e^+e^- \rightarrow t\bar{c} e^+e^-)$ using the effective vector boson approximation (EVBA) [24]. In this approximation, as in the equivalent photon approximation in QED, the colliding W 's or Z 's are treated as on shell particles and, thus, the salient features of the $2 \rightarrow 4$ reactions $e^+e^- \rightarrow t\bar{c} \nu_e \bar{\nu}_e$, $t\bar{c} e^+e^-$ are generated by the simpler $2 \rightarrow 2$ subprocesses W^+W^- , $ZZ \rightarrow t\bar{c}$. The full $2 \rightarrow 4$ cross sections $\sigma_{V_1 V_2}$ ($V_1, V_2 = W^+, W^-$ or $V_1, V_2 = Z, Z$) are estimated by folding in the distribution functions $f_{V_1}^{\lambda_1}, f_{V_2}^{\lambda_2}$ of the two colliding V_1, V_2 with helicities λ_1, λ_2 [24], explicitly,

$$\sigma_{V_1 V_2} = \sum_{\lambda_1, \lambda_2} \int dx_1 dx_2 f_{V_1}^{\lambda_1}(x_1) f_{V_2}^{\lambda_2}(x_2) \hat{\sigma}(V_1^{\lambda_1} V_2^{\lambda_2} \rightarrow t\bar{c}). \quad (34)$$

We find that $\sigma_{ZZ} \lesssim 10^{-3}$ fb at $\sqrt{s} = \Lambda = 1.5$ TeV, for $a_L^Z = 1$ or $a_R^Z = 1$, and is therefore too small to be observed. However, σ_{WW} is typically about two orders of magnitude larger, partly because in this approximation the W -boson luminosity is larger than the luminosity for the Z -bosons due to different couplings to electrons (see e.g., [25]). In particular, we find $\sigma_{WW} \sim 0.15$ (0.09) fb at $\sqrt{s} = \Lambda = 1.5$ (2) TeV, for $a_L^Z = 1$, $a_R^Z = 0$ or $a_L^Z = 0$, $a_R^Z = 1$. Comparing with $\sigma(e^+e^- \rightarrow Z \rightarrow t\bar{c} + t\bar{c}) \sim 0.14$ (0.03) fb for the same values of \sqrt{s} , Λ and $a_{L,R}^Z$, we see that the WW -fusion process is a slightly more sensitive probe of such new Ztc couplings at these high c.m. energies.⁶

Let us now return to the four-Fermi case; we wish to explore the limits that can be obtained on the scale Λ of such four-Fermi operators in the case that no $e^+e^- \rightarrow t\bar{c}$ events are observed. To do so we first consider the possible observable final states for this reaction:

(1) If the top decays hadronically via $t \rightarrow bW^+ \rightarrow b j_1 j_2$, where j_1, j_2 are light jets coming from $W^+ \rightarrow u\bar{d}$ or $c\bar{s}$, then we have $e^+e^- \rightarrow t\bar{c} \rightarrow b\bar{c} j_1 j_2$ (and $e^+e^- \rightarrow t\bar{c} \rightarrow \bar{b}c j_1 j_2$ for the charge conjugate channel). These final states occur with a branching ratio of 2/3.

(2) If the top decays semi-leptonically via $t \rightarrow bW^+ \rightarrow b l^+ \nu_l$, where $l = e, \mu$ or τ , then we have $e^+e^- \rightarrow b\bar{c} l^+ \nu_l$ (and $e^+e^- \rightarrow \bar{b}c l^- \bar{\nu}_l$ for the charge conjugate channel). These final states occur with a branching ratio of 1/3.

An immediate useful observation is that each of the two top decay scenarios above contains a single b -jet in the final state, which can be used as a signal for non-SM physics [15]. Indeed, SM reactions in lepton colliders produce almost exclusively final states with an *even* number of b -jets. Defining a quantum number we called $b_p = (-1)^n$, where n is the number of b -jets in the final state, the SM is almost exclusively b_p -even. The SM irreducible background to b_p -odd processes generated by new physics is severely suppressed by off-diagonal CKM elements and can be neglected. The only remaining (reducible) background to processes which yield an odd number of b -jets in the final state arises from mis-identifying an odd number of b -jets in a b_p -even event [15].

For the process $e^+e^- \rightarrow t\bar{c}$, the SM irreducible background is generated, for example, by $e^+e^- \rightarrow W^+W^-$ followed by $W^+ \rightarrow j_1 j_2$ and $W^- \rightarrow b\bar{c}$ for hadronic top decays (case 1 above) or by $W^+ \rightarrow l^+ \nu_l$ and $W^- \rightarrow b\bar{c}$ for semi-leptonic top decays (case 2 above), see also [17]. These backgrounds are clearly CKM suppressed, being $\propto |V_{cb}|^2$, and can therefore be neglected.

⁶We recall that, at these high c.m. energies ($\sqrt{s} = 1.5 - 2$ TeV), the projected integrated luminosity is expected to be several hundreds inverse fb, see Ref. [1]. Thus, a cross section of the order of 0.1 fb may yield an observable effect, especially for the rather unique $t\bar{c}$ final state which has a negligible background as we discuss below.

TABLE I. The limits on the scale of the new physics Λ using the reaction $e^+e^- \rightarrow t\bar{c} + \bar{t}c$. The limits are given for one non-vanishing coupling at a time and setting this coupling to 1. In each case four accelerator scenarios are considered; $\sqrt{s} = 189, 200, 500$ and 1000 GeV with luminosities $L = 0.6, 2.5, 50$ and 200 fb $^{-1}$, respectively. The signals considered are based on the total cross section as defined in (35), assuming a b -tagging efficiency of 60% and a top reconstruction efficiency of 80% (see text). Also, the limits are based on the criterion of 10 events for the given luminosity.

Limits from $\bar{\sigma}_{tc} = \epsilon_b \epsilon_t \sigma(e^+e^- \rightarrow t\bar{c})$					
\sqrt{s}	L	$a_i^Z = 1$ $i = L$ or R	$V_{ij} = 1$ $ij = LL, LR, RR$ or RL	$S_{RR} = 1$	$T_{RR} = 1$
189 GeV	0.6 fb $^{-1}$	0.5 TeV	0.8 TeV	0.7 TeV	1.4 TeV
200 GeV	2.5 fb $^{-1}$	0.9 TeV	1.5 TeV	1.3 TeV	2.5 TeV
500 GeV	50 fb $^{-1}$	1.9 TeV	9.3 TeV	8.5 TeV	13.6 TeV
1000 GeV	200 fb $^{-1}$	2.0 TeV	19.3 TeV	17.9 TeV	27.5 TeV

In order to further eliminate the reducible background to b_p -odd events produced by a b -tagging efficiency below 1, one can employ a few more specific experimental handles allowed by the very distinct characteristics of a $t\bar{c}$ signature: (i) The possibility of efficiently reconstructing the t from the decay $t \rightarrow bW \rightarrow bj_1j_2$ at the NLC [26]; the top quark can also be reconstructed in the case of semi-leptonic top decays since there is only one missing neutrino in such a $t\bar{c}$ event. (ii) Since this is a $2 \rightarrow 2$ process, the two-body kinematics fixes the charm-jet energy to be $E_c \simeq \sqrt{s}(1 - m_t^2/s)/2$. The charm-jet gives then a unique signal since it recoils against the massive top quark and should stand out as a very energetic light jet at high c.m. energies. The event will then look like a single top quark event. (iii) The energy of the b -jet produced in top decay is also known due to two-body kinematics [17].

Let us therefore define our background-free observable cross section, which we denote by $\bar{\sigma}_{tc}$, as the effective cross section including b -tagging efficiency (ϵ_b) and top quark reconstruction efficiency (ϵ_t)

$$\bar{\sigma}_{tc} = \epsilon_b \epsilon_t \sigma_{tc}. \quad (35)$$

We define the largest Λ to which a collider is sensitive as the one for which 10 fully reconstructed $t\bar{c} + \bar{t}c$ events are generating per year, after eliminating any potential background, i.e., the value of Λ for which $\bar{\sigma}_{tc} \times L = 10$, where L is the yearly integrated luminosity of the given collider.

In Table I we list the limits that can be placed on the scale Λ of the new effective four-Fermi and Ztc operators, based on this 10 event criterion, using the background-free cross section as defined in Eq. (35); we take $\epsilon_b = 60\%$ and $\epsilon_t = 80\%$ and we impose a 10° angular cut on the c.m. scatter-

ing angle.⁷ The limits are calculated, assuming that only one coupling is non-vanishing at a time, i.e., with either $V_{ij} = 1$, for $i, j = LL$ or LR or RR or RL , or $S_{RR} = 1$ or $T_{RR} = 1$ or $a_L^Z = 1$. We give the limits that may already be obtainable from the recent 189 GeV run of LEP2 which accumulated ~ 150 inverse pb in each of the four LEP2 detectors [27]. We also consider three future collider scenarios: LEP2 with a c.m. energy of $\sqrt{s} = 200$ GeV and an integrated luminosity of $L = 2.5$ fb $^{-1}$, a NLC with $\sqrt{s} = 500$ GeV and $L = 50$ fb $^{-1}$ and a NLC with $\sqrt{s} = 1000$ GeV and $L = 200$ fb $^{-1}$. As expected, the strongest limits are obtained using the four-Fermi couplings. In particular, assuming that no $t\bar{c}$ event was seen during the recent LEP2 run, this rules out new flavor physics (that can generate such four-Fermi operators) up to energy scales of $\Lambda \gtrsim 0.7 - 1.4$ TeV. For the future e^+e^- machines, the limits on the scale of the four-Fermi operators are typically $\Lambda \gtrsim 7 - 12 \times \sqrt{s}$ for LEP2 energies and $\Lambda \gtrsim 17 - 27 \times \sqrt{s}$ for a 500 or 1000 GeV NLC. The best limits are obtained on the tensor four-Fermi coupling T_{RR} due to numerical factors in the cross section.

The above results were obtained assuming that all couplings were equal to 1, for other values the the limits in Table I are in fact on Λ/\sqrt{f} , where $f = V, S, T$ or a^Z . To illustrate this possibility consider, for example, the tensor four-Fermi coupling which can (of course) be generated by the exchange of a heavy neutral tensor excitation, of mass Λ .

⁷We note that our limits on the scale of the Ztc operator are more stringent than those obtained in [17]. This difference arises from our assumption that once the top quark is reconstructed (with an efficiency of $\epsilon_b \times \epsilon_t$) and the charm jet is identified (as described above), there is no additional background to be considered for the tc final state; the results of [17] obtained using a more careful background estimate correspond to a reduced reconstruction efficiency of $\epsilon_b \epsilon_t = 42\%$ instead of 48% which we used.

But this effective vertex is also generated through Fierz-transforming the operator $\mathcal{O}_{lq'}$ in Eq. (23), which can be produced by the exchange of a heavy scalar leptoquark in the underlying high energy theory. In the latter case the coefficient T_{RR} has an additional factor of 1/8, so that the mass of the leptoquark corresponds to $\sqrt{8}\Lambda$. These two possibilities cannot be easily differentiated using an effective theory and provide an example of the limitations of this parametrization.

It is also instructive to note that, in case a $t\bar{c}$ signal is observed, there are enough independent observables in the

reaction $e^+e^- \rightarrow t\bar{c}$ to allow the extraction of all 6 independent four-Fermi couplings discussed above. These observables are, for example, the cross sections for polarized electrons and for definite top polarization (viable in the semi-leptonic [28] and in the hadronic top decays if the down quark jet can be distinguished from the up quark jet in $W \rightarrow du$ [29]), and the following forward-backward (FB) asymmetries for polarized incoming electrons (i.e., for the reactions $e_L^-e^+ \rightarrow t\bar{c}$ and $e_R^-e^+ \rightarrow t\bar{c}$)

$$A_{FB_L} = \frac{\int_0^{\pi/2} \{d\sigma_{e_L^+t_L}(\theta) + d\sigma_{e_L^+t_R}(\theta) - d\sigma_{e_L^+t_L}(\pi-\theta) - d\sigma_{e_L^+t_R}(\pi-\theta)\}}{\sigma_{e_L^+t_L} + \sigma_{e_L^+t_R}} = \frac{3(1+\beta_t)}{2(3+\beta_t)} \frac{V_{LR}^2 - V_{LL}^2}{V_{LR}^2 + V_{LL}^2}, \quad (36)$$

$$A_{FB_R} = \frac{\int_0^{\pi/2} \{d\sigma_{e_R^+t_L}(\theta) + d\sigma_{e_R^+t_R}(\theta) - d\sigma_{e_R^+t_L}(\pi-\theta) - d\sigma_{e_R^+t_R}(\pi-\theta)\}}{\sigma_{e_R^+t_L} + \sigma_{e_R^+t_R}} \\ = \frac{3(1+\beta_t)[V_{RL}^2 - V_{RR}^2 + 4S_{RR}T_{RR}]}{2(3+\beta_t)[V_{RL}^2 + V_{RR}^2 + 3(1+\beta_t)S_{RR}^2 + 16(3-\beta_t)T_{RR}^2]}. \quad (37)$$

Clearly, the FB asymmetries involve ratios of cross sections and, therefore, are not suppressed by inverse powers of Λ . A detailed discussion of how to extract the six four-Fermi couplings from such observables lies outside the scope of this paper; we limit ourselves to the summary of the sensitivity of each observable as presented in Table II.

We conclude this section with a few remarks.

Some of the four-Fermi effective operators in Eqs. (17)–(23), that generate the new $tcee$ coupling also induce inter-

TABLE II. The sensitivity of the different observables discussed in the text to the various new four-Fermi effective couplings. The observables considered are the polarized cross sections $\sigma_{e_i^+t_j}$, $i, j = LL, LR, RR, RL$ in Eqs. (27)–(30) and the FB asymmetries A_{FB_L} and A_{FB_R} for left and right-handed incoming electron beam, respectively, as defined in Eqs. (36) and (37). A check-mark shows that the given observable is sensitive to the given coupling.

Observables vs. Couplings						
	$\sigma_{e_L^+t_L}$	$\sigma_{e_L^+t_R}$	$\sigma_{e_R^+t_L}$	$\sigma_{e_R^+t_R}$	A_{FB_L}	A_{FB_R}
V_{LL}	✓	✓			✓	
V_{LR}	✓	✓			✓	
V_{RR}			✓	✓		✓
V_{RL}			✓	✓		✓
S_{RR}			✓			✓
T_{RR}			✓	✓		✓

actions involving the down quarks of the second and third generations. For example, the operators $\mathcal{O}_{lq}^{(1)}$ and $\mathcal{O}_{lq}^{(3)}$, being constructed out of the left-handed quark doublets, will generate a $t\bar{c}e^+e^-$ interaction [with coupling $\alpha_{lq}^{(1)} - \alpha_{lq}^{(3)}$, see Eq. (25)] as well as a $b\bar{s}e^+e^-$ one with coupling $\alpha_{lq}^{(1)} + \alpha_{lq}^{(3)}$. This fact, a consequence of gauge invariance, can be used to derive constraints on the scale Λ . For example, using the measured B^+ semi-leptonic branching ratio, such four-Fermi operators contributions to $B^+ \rightarrow K^+ e^+ e^-$ will be below the existing bound $\text{Br}(B^+ \rightarrow K^+ e^+ e^-) < 10^{-5}$ [30], provided that $\Lambda/\sqrt{|\alpha_{lq}^{(1)} + \alpha_{lq}^{(3)}|} \geq 2$ TeV. Due to the different combination of couplings appearing in this expression this bound is complementary to the ones obtained above.

We wish to emphasize the importance of adding such possible four-Fermi interactions to a model independent analysis of $e^+e^- \rightarrow t\bar{c}$. We argued previously that the only models that can produce observable flavor violations are those which generate flavor-changing operators at tree-level. In this case the effective Ztc vertex is generated by the exchange of a heavy gauge boson V which mixes with the Z and which has a Vtc vertex (this vertex is also produced by heavy fermion exchanges). Similarly, some of the four-Fermi operators are generated by the exchange of a heavy vector V' coupling to $t\bar{c}$ and to e^+e^- . In general we have $V' \neq V$ so that an analysis that covers all the possibilities allowed by an effective Lagrangian parametrization should include both types of vertices. If, on the other hand $V=V'$, then the bounds obtained from the four-Fermi contact interactions are far superior to the ones derived from Z -mediated reactions. In this case V

would also generate a $eeee$ contact interaction for which existing limits [30] give $\Lambda \gtrsim 1.5$ TeV, i.e., better than the limits given in Table I for a 189 GeV LEP2. We note, however, that at a 500 GeV NLC the limits that can be obtained on the $eeee$ contact terms by studying the reaction $e^+e^- \rightarrow e^+e^-$ are about $\Lambda > 5$ TeV [21], while from Table I we see that $\Lambda > 8.5\text{--}13.6$ TeV is attainable at this energy by studying the process $e^+e^- \rightarrow t\bar{c}$.

We would like to stress again that the limits obtained in Table I presuppose the heavy physics does generate the four-Fermi operators at an accessible scale. Other types of new physics can be responsible for generating the Ztc vertex, raising the possibility that the latter occurs even when the former is negligible. In that sense, the above results are complementary to those obtained e.g., in [13].

IV. EFFECTIVE FLAVOR-CHANGING SCALAR INTERACTIONS AND $T\bar{c}$ PRODUCTION AT A NLC

In this section we consider neutral Higgs exchanges in the NLC which lead to $t\bar{c}$ production via a new htc interaction as defined in Sec. II [see Eqs. (11) and (12)]. We neglect $2 \rightarrow 3$ (i.e., three-body final state) processes since these are suppressed by phase space compared to $2 \rightarrow 2$ processes.

There are only two such reactions that can probe an effective htc vertex in e^+e^- colliders. The first is the Bjorken process $e^+e^- \rightarrow Zh$ when a real Higgs boson is produced and then decay to a $t\bar{c}$ pair (see Fig. 2), and the second is the t -channel W^+W^- -fusion to a neutral Higgs boson in Fig. 3(b), leading to $e^+e^- \rightarrow W^+W^- \nu_e \bar{\nu}_e \rightarrow t\bar{c} \nu_e \bar{\nu}_e$. We note that the corresponding t -channel ZZ -fusion process $e^+e^- \rightarrow ZZ e^+e^- \rightarrow t\bar{c} e^+e^-$, also depicted in Fig. 3(b), is about an order of magnitude smaller than the WW -fusion process, basically, due to the different couplings of a Z -boson to electrons (see also the discussion in the previous section).

We focus on Higgs masses in the range $m_t \lesssim m_h \lesssim 500$ GeV. Since at this mass range the neutral Higgs width is still quite small compared to its mass, e.g., for $m_h = 250(500)$ GeV the width is about 1.5% (13%) of its mass, and since we only consider real Higgs production, we may estimate the cross section for $e^+e^- \rightarrow Zt\bar{c}$ by

$$\sigma_{Ztc} = \sigma(e^+e^- \rightarrow Zt\bar{c}) \approx \sigma(e^+e^- \rightarrow Zh) \times \text{Br}(h \rightarrow t\bar{c}), \quad (38)$$

where [25]

$$\sigma(e^+e^- \rightarrow Zh) = \frac{\pi\alpha^2}{192c_W^4 s_W^4} [1 + (1 - 4s_W^2)^2] \frac{8\kappa(\kappa^2 + 3m_Z^2)}{\sqrt{s}(s - m_Z^2)}, \quad (39)$$

and

$$\kappa = \sqrt{\frac{(s + m_Z^2 - m_h^2)^2 - 4sm_Z^2}{4s}}. \quad (40)$$

Using now

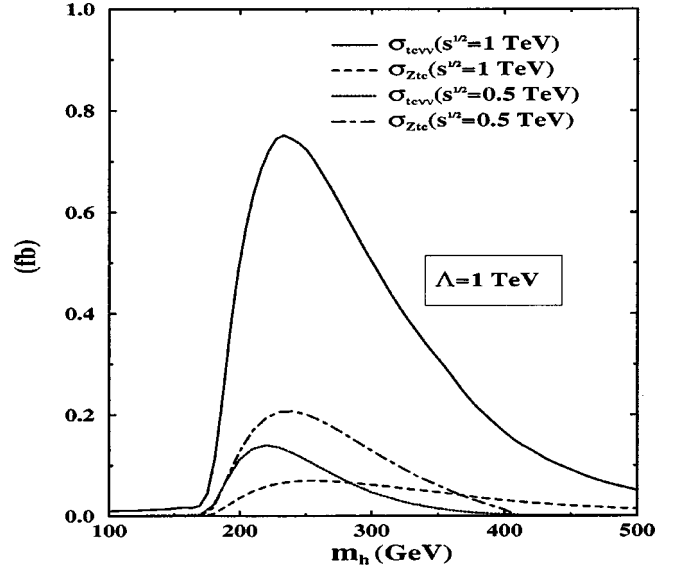


FIG. 6. The cross sections $\sigma_{Ztc} = \sigma(e^+e^- \rightarrow Zt\bar{c} + Z\bar{t}c)$ and $\sigma_{tc\nu\nu} = \sigma(e^+e^- \rightarrow t\bar{c}\nu_e\bar{\nu}_e + \bar{t}c\nu_e\bar{\nu}_e)$ (in fb) are plotted as a function of the SM Higgs mass m_h , for an e^+e^- collider with a c.m. energy of $\sqrt{s} = 500$ GeV (dotted and dot-dashed lines) and of $\sqrt{s} = 1000$ GeV (solid and dashed lines). $\Lambda = 1$ TeV is used for all cases.

$$\text{Br}(h \rightarrow t\bar{c}) = \frac{\Gamma(h \rightarrow t\bar{c})}{\Gamma_h}, \quad (41)$$

where $\Gamma_h = \Gamma(h \rightarrow b\bar{b}) + \Gamma(h \rightarrow ZZ) + \Gamma(h \rightarrow W^+W^-) + \Gamma(h \rightarrow t\bar{t})$ is the total SM Higgs width,⁸ see e.g., [31], and $\Gamma(h \rightarrow t\bar{c})$ is calculated in terms of the new htc couplings a_L^h and a_R^h defined in Eq. (11), we find

$$\Gamma(h \rightarrow t\bar{c}) = \frac{v^4}{\Lambda^4} \frac{3\alpha}{4s_W^2} [(a_L^h)^2 + (a_R^h)^2] m_h \left(1 - \frac{m_t^2}{m_h^2}\right)^2. \quad (42)$$

For this type of effective vertices we also calculate the t -channel fusion cross section $\sigma_{tc\nu\nu} = \sigma(e^+e^- \rightarrow t\bar{c}\nu_e\bar{\nu}_e)$ using the EVBA [24] (see also the previous section). The amplitude for the hard $2 \rightarrow 2$ sub-process $W_\lambda^+ W_\lambda^- \rightarrow h \rightarrow t\bar{c}$ with c.m. energy \sqrt{s} is given by

$$\begin{aligned} \mathcal{M}_{\lambda^+, \lambda^-} &= \frac{v^2}{\Lambda^2} \frac{\pi\alpha}{s_W^2} \hat{s} \sqrt{1 - \beta_W^2} \sqrt{\frac{2\beta_t}{1 + \beta_t}} \Pi_h \delta_{\lambda_t, \lambda_c} T_{\lambda^+, \lambda^-} \\ &\times [a_L^h(1 + \lambda_t) - a_R^h(1 - \lambda_t)], \end{aligned} \quad (43)$$

where $\lambda^+, \lambda^- = 0, \pm 1$ are the helicities of the W^+, W^- , respectively, and $\lambda_{t,c} = \pm 1/2$ denote the quark helicities. Also,

⁸ $h \rightarrow t\bar{t}$ and $h \rightarrow ZZ$ are included when kinematically allowed.

$\Pi_h = (\hat{s} - m_h^2 + im_h\Gamma_h)^{-1}$ is the Higgs propagator, $\beta_t = (\hat{s} - m_t^2)/(\hat{s} + m_t^2)$, $\beta_W = \sqrt{1 - 4m_W^2/\hat{s}}$ and

$$T_{0,0} = \frac{1 + \beta_W^2}{1 - \beta_W^2},$$

$$T_{\pm,\pm} = 1, \quad (44)$$

$$T_{\pm,\mp} = T_{\pm,0} = T_{0,\pm} = 0.$$

The polarized (with respect to the W^+ and W^-) hard cross section $\hat{\sigma}(W_{\lambda^+}^+ W_{\lambda^-}^- \rightarrow h \rightarrow t\bar{c})$ can then be readily calculated. From this expression the cross section $\sigma_{tc\nu\nu}$ is again estimated by folding in the distribution functions $f_{W^+}^{\lambda^+}, f_{W^-}^{\lambda^-}$ of the two colliding W^+, W^- in a given helicity state λ^+, λ^- as in Eq. (34)

$$\sigma_{tc\nu\nu} = \sum_{\lambda^+\lambda^-} \int dx_+ dx_- f_{W^+}^{\lambda^+}(x_+) f_{W^-}^{\lambda^-}(x_-)$$

$$\times \hat{\sigma}(W_{\lambda^+}^+ W_{\lambda^-}^- \rightarrow h \rightarrow t\bar{c}). \quad (45)$$

The bulk contribution to the full $2 \rightarrow 4$ process arises when the Higgs resonates, i.e., when $\sqrt{\hat{s}} \sim m_h$ ($\sqrt{\hat{s}}$ denotes the c.m. energy of the hard $2 \rightarrow 2$ process). Because of this, $\text{Br}(h \rightarrow t\bar{c})$ also controls the dependence of this WW -fusion reaction on the Higgs mass. This behavior is illustrated in Fig. 6 in which we plot σ_{Ztc} and $\sigma_{tc\nu\nu}$ as a function of m_h for c.m. energies of 500 and 1000 GeV. In this figure we take $a_L^h = a_R^h = 1$ and $\Lambda = 1$ TeV. We see that these cross sections reach their maximum for $m_h \sim 230$ GeV, close to the value at which $\text{Br}(h \rightarrow t\bar{c})$ is largest.

We now discuss these signals and their observability in future high energy e^+e^- colliders. From Fig. 6 we see that, at c.m. energy of 500 GeV, the Bjorken process dominates, giving $\sigma_{Ztc} \sim 0.2$ fb for $m_h \sim 250$ GeV, $a_L^h = a_R^h = 1$ and $\Lambda = 1$ TeV. In Fig. 7 we plot σ_{Ztc} and $\sigma_{tc\nu\nu}$ as a function of the e^+e^- c.m. energy \sqrt{s} , for $m_h = 250$ GeV, $a_L^h = a_R^h = 1$ and $\Lambda = 1$ or 2 TeV. Since $\sigma_{tc\nu\nu}$ is a t -channel fusion process, it grows logarithmically as $\sim \log^2(s/m_W^2)$ and, therefore, dominates at higher energies over the s -channel Bjorken process which drops as $\sim 1/s$. For example, at $\sqrt{s} = 1$ TeV and $m_h \sim 250$ GeV we find $\sigma_{tc\nu\nu}/\sigma_{Ztc} \sim 10$.

In order to identify the background to these reactions, we follow the same approach described in the previous section. We consider the possible observable final states in $e^+e^- \rightarrow Zt\bar{c}$ (assuming that the Z is identified with 100% efficiency) and $e^+e^- \rightarrow t\bar{c}\nu_e\bar{\nu}_e$, which are determined by the top decays. For hadronic top decays we have $e^+e^- \rightarrow Zt\bar{c} \rightarrow Z\bar{c}bj_1j_2$ and $e^+e^- \rightarrow t\bar{c}\nu_e\bar{\nu}_e \rightarrow \bar{c}bj_1j_2\nu_e\bar{\nu}_e$, where j_1 and

j_2 are light jets from $W^+ \rightarrow u\bar{d}$ or $W^+ \rightarrow c\bar{s}$. For the semi-leptonic top decays we have $e^+e^- \rightarrow Zt\bar{c} \rightarrow Z\bar{c}bl^+\nu_l$ and $e^+e^- \rightarrow t\bar{c}\nu_e\bar{\nu}_e \rightarrow \bar{c}bl^+\nu_l\nu_e\bar{\nu}_e$, where $l = e, \mu$ or τ from $W^+ \rightarrow l^+\nu_l$.

Since only one top quark is produced, these final states have one b -jet so that they have a negligible irreducible background, as mentioned previously. There is, as before, a potentially dangerous reducible SM background due to a reduced b -tagging efficiency ϵ_b . For example, such a background is generated by the reaction $e^+e^- \rightarrow Zh$ when h decays into a $t\bar{t}$ pair (assuming $m_h > 2m_t$) and one b quark in the top decay products is not detected. Similarly, for $e^+e^- \rightarrow t\bar{c}\nu_e\bar{\nu}_e$ the SM reducible background is generated by processes such as $e^+e^- \rightarrow W^+W^- \nu_e\bar{\nu}_e, t\bar{t}\nu_e\bar{\nu}_e$ (see also [7] and Hou *et al.* in [11]). Recall, however, that as in the case of $e^+e^- \rightarrow t\bar{c}$, a $t\bar{c}$ signal has more experimental handles such as top reconstruction, a very energetic charm-jet, etc. and these can be used to eliminate most of the background events.

To obtain limits on the scale of the new physics, Λ , we again define the background-free cross sections, $\bar{\sigma}_{Ztc}$ and $\bar{\sigma}_{tc\nu\nu}$, by folding the b -tagging and top reconstruction efficiency factors, which essentially eliminate the type of reducible backgrounds mentioned above. Thus, our background-free observable cross sections are

$$\bar{\sigma}_{tc\nu\nu} = \frac{2}{3} \epsilon_b \epsilon_t \sigma_{tc\nu\nu}, \quad \bar{\sigma}_{Ztc} = \epsilon_b \epsilon_t \sigma_{Ztc}, \quad (46)$$

where the factor of $2/3$ in the cross section for the $t\bar{c}\nu_e\bar{\nu}_e$ reaction takes into account the fact that only the hadronic top decay, $t \rightarrow bj_1j_2$ are useful (we assume that the semi-leptonic

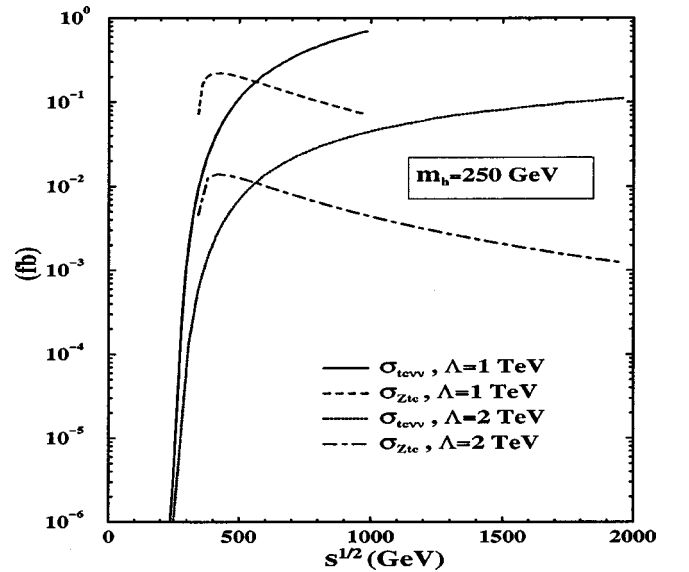


FIG. 7. The cross sections $\sigma_{Ztc} = \sigma(e^+e^- \rightarrow Zt\bar{c} + Z\bar{t}c)$ and $\sigma_{tc\nu\nu} = \sigma(e^+e^- \rightarrow t\bar{c}\nu_e\bar{\nu}_e + \bar{t}c\nu_e\bar{\nu}_e)$ (in fb) are plotted as a function of the c.m. energy of the e^+e^- collider, for $m_h = 250$ GeV and for: $\Lambda = 1$ TeV (solid and dashed lines) and $\Lambda = 2$ TeV (dotted and dot-dashed lines). See also text.

⁹Notice that some of the lines end rather abruptly whenever $\sqrt{s} = \Lambda$, since for $\Lambda < \sqrt{s}$ the effective Lagrangian description is not valid by definition.

TABLE III. Limits on the scale, Λ , of the new physics that generates new htc effective operators, using the reactions $e^+e^- \rightarrow t\bar{c}\nu_e\bar{\nu}_e + \bar{t}c\nu_e\bar{\nu}_e$ and $e^+e^- \rightarrow Zt\bar{c} + Z\bar{t}c$ (in parentheses). The limits are given for $m_h = 200, 250$, and 400 GeV where in each case three accelerator scenarios are considered; $\sqrt{s} = 500, 1000$ and 1500 GeV with luminosities $L = 50, 200$ and 500 fb^{-1} , respectively. The signals considered are based on the total cross sections, as defined in (46), assuming a b -tagging efficiency of 60% and a top reconstruction efficiency of 80%. The limits are based on our criterion of 10 events for the given luminosity and the given reaction (see also text).

		Limits from $\{\bar{\sigma}_{t\nu\nu}, \bar{\sigma}_{Ztc}\}$		
		$m_h = 200$ GeV	$m_h = 250$ GeV	$m_h = 400$ GeV
\sqrt{s}	L			
500 GeV	50 fb^{-1}	{650, 750} GeV	{650, 830} GeV	{X, X} GeV
1000 GeV	200 fb^{-1}	{1340, X} GeV	{1460, X} GeV	{1010, X} GeV
1500 GeV	500 fb^{-1}	{1930, X} GeV	{2140, X} GeV	{1600, X} GeV

top decays cannot be reconstructed due to the additional two missing neutrinos in the final state). As before, we assume that the largest value of Λ which can be probed using these processes corresponds to the value yielding a signal of 10 fully reconstructed events.

In Table III we give the 3σ limits that can be placed on the scale of the new physics Λ using the processes $e^+e^- \rightarrow Zt\bar{c} + Z\bar{t}c$ and $e^+e^- \rightarrow t\bar{c}\nu_e\bar{\nu}_e + \bar{t}c\nu_e\bar{\nu}_e$, assuming no signal is observed (based on our 10 event criterion); we take $\epsilon_b = 60\%$, $\epsilon_t = 80\%$ and $a_L^h = a_R^h = 1$. We consider three collider scenarios: a NLC with $\sqrt{s} = 500$ GeV and a yearly integrated luminosity of $L = 50$ fb^{-1} , $\sqrt{s} = 1000$ GeV with $L = 200$ fb^{-1} and $\sqrt{s} = 1500$ GeV with $L = 500$ fb^{-1} . Entries marked by an X in Table III indicate the cases for which no interesting limit can be obtained, i.e., where the limit corresponds to $\Lambda < \sqrt{s}$. Because of its decreasing nature, the cross section $e^+e^- \rightarrow Zt\bar{c} + Z\bar{t}c$ is only useful at 500 GeV, for which a limit of e.g., $\Lambda \geq 830$ GeV is obtainable if $m_h \sim 250$ GeV. Using the $t\bar{c}\nu_e\bar{\nu}_e + \bar{t}c\nu_e\bar{\nu}_e$ final state, one can place the limits $\Lambda \geq 1460$ GeV and $\Lambda \geq 2140$ GeV in a 1000 GeV and 1500 GeV NLC, respectively (with $m_h \sim 250$ GeV). Note that these limits are weakened if $m_h = 200$ or 400 GeV, since these cross sections are smaller for such Higgs boson mass values (see Fig. 6).

V. RIGHT-HANDED Wtb EFFECTS IN $W^+W^- \rightarrow t\bar{c}$

The WW -fusion process $W^+W^- \rightarrow t\bar{c}$ can proceed at the tree-graph level in the SM via diagram (c) in Fig. 3. The cross section, however, is unobservably small due to GIM suppression: $\sigma_{t\nu\nu} \sim \text{few} \times 10^{-4}$ fb at a NLC with c.m. energies in the range 1–2 TeV (see also [7]).

This suppression opens the possibility of observing a $t\bar{c}\nu_e\bar{\nu}_e$ signal in the presence of an effective right-handed Wtb coupling, $\delta_{R,b}^t$, defined in Eq. (16). We consider these effects on the reaction $e^+e^- \rightarrow W^+W^- \nu_e\bar{\nu}_e \rightarrow t\bar{c}\nu_e\bar{\nu}_e + \bar{t}c\nu_e\bar{\nu}_e$, which we evaluate using the EVBA.

We find, however, that the effective interactions do not

produce a significant enhancement in these cross sections since $\delta_{R,b}^t \leq 1$ (resulting from $\alpha_{\phi\phi}$). The reason follows from the structure of the amplitude, \mathcal{M}_{Wtd_i} , for $W^+W^- \rightarrow t\bar{c}$ calculated using Eq. (16)

$$\begin{aligned} \mathcal{M}_{Wtd_i} \propto m_i [& C_{LL}(V_{ti} + \delta_{L,i}^t)(V_{ci}^* + \delta_{L,i}^c) + C_{RR}\delta_{R,i}^t\delta_{R,i}^c] \\ & + m_d [C_{LR}(V_{ti} + \delta_{L,i}^t)\delta_{R,i}^c + C_{RL}\delta_{R,i}^t(V_{ci}^* + \delta_{L,i}^c)], \end{aligned} \quad (47)$$

where C_{LL} , C_{RR} , C_{LR} and C_{RL} are some kinematic functions with a mass dimension -1 . If the only non-vanishing effective coupling is $\delta_{R,b}^t$, then the amplitude is proportional to the very small SM off-diagonal CKM element V_{cb} and, in addition, it contains a mass insertion factor m_b from the t -channel b -quark propagator [see Fig. 3(c)]. If in addition $\delta_{R,b}^c \neq 0$, then the amplitude receives also a contribution proportional to $\delta_{R,b}^t \times \delta_{R,b}^c$ (with no mass insertion). However, such a term will give a cross section which is proportional to v^8/Λ^8 instead of v^4/Λ^4 and is, therefore, also very small. We conclude that such right-handed current effects cannot be probed via the WW -fusion process.

Before summarizing we wish to note that the hard cross section $W^+W^- \rightarrow t\bar{c}$ needed in the EVBA exhibits a *physical* t -channel singularity [32]. Due to the specific kinematics of this $2 \rightarrow 2$ process, the square of the t -channel momentum can be positive and the down quark propagator can, therefore, resonate once $t \sim m_d^2$. The reason for that is rather clear: the incoming W -boson can decay to an on-shell pair of $d_i\bar{c}$ ($d_i = d, s$ or b). The singularity, therefore, signals the production of an on-shell down quark in the t -channel.

The t -channel singularity of the $2 \rightarrow 2$ sub-process does not occur in the full $2 \rightarrow 4$ process. In the exact calculation, i.e., without using the EVBA, the exchanged W^+ and W^- cannot be on-shell since the W^+ , W^- momenta are always space-like; as a consequence the Q^2 of the t -channel down

quark is always negative.¹⁰ Therefore, the EVBA, which assumes on-shell incoming vector-bosons, breaks down in such situations and cannot be used to approximate these type of processes. To bypass this problem, we have used the EVBA with massless incoming W -bosons when calculating the above cross sections. We have checked that such an additional approximation gives rise to an error of the order of $\sim m_W/\sqrt{s}$ which is less than 10% for a c.m. energy of $\sqrt{s} = 1000$ GeV.

VI. SUMMARY

We have considered production of a $t\bar{c}$ pair in e^+e^- colliders in the effective Lagrangian description. We investigated a variety of processes, leading to a $t\bar{c}$ signal, which may be driven by some underlying flavor physics beyond the SM that gives rise to new vertices such as Ztc , htc , right-handed Wtb and four-Fermi $tcee$ interactions.

We have shown that, if present, the contributions of four-Fermi operators strongly dominate the cross section for the reaction $e^+e^- \rightarrow t\bar{c}$, while the effects of flavor-changing Z vertices are subdominant, assuming both types of effective operators appear with coefficients of order one (which is the case in all natural theories) and of similar scales though, as was mentioned previously, these two types of vertices may probe different kinds of physics and, therefore, should be measured separately.

Thus, the Ztc vertex may alternatively be probed via the t -channel WW -fusion process $W^+W^- \rightarrow t\bar{c}$ which may yield an observable $t\bar{c}\nu_e\bar{\nu}_e$ signal at 1.5–2 TeV e^+e^- linear colliders. At hadron colliders the Ztc vertex can also be efficiently probed in flavor changing top decays [33], and in single top production in association with a Z -boson [34].

The t -channel WW -fusion process was also found to be

sensitive to new htc scalar interactions which may also lead to a $t\bar{c}\nu_e\bar{\nu}_e$ signal at 1–2 TeV NLC. We showed, however, that, at c.m. energies below 1 TeV, effective htc couplings are better probed via the Bjorken process $e^+e^- \rightarrow Zh$ followed by $h \rightarrow t\bar{c}$.

The effects of a new right-handed Wtb coupling were found to be negligible for $t\bar{c}$ production in e^+e^- colliders in WW -fusion processes.

We have argued that, due to its unique characteristics, the $t\bar{c}$ final state is essentially free of SM irreducible background and may be, therefore, easily identified in an e^+e^- collider environment. In addition, by tagging the single b -jet coming from $t \rightarrow bW$ and by reconstructing the top quark from its decay products one is able, in principle, to eliminate all possible SM reducible background to the $t\bar{c}$ signal.

Using reasonable b -jet tagging and top reconstruction efficiencies at e^+e^- colliders, we have derived sensitivity limits for these machines to the scale of new flavor-changing physics, Λ . For example, we find that an absence of a $e^+e^- \rightarrow t\bar{c}$ signal at the recent 189 GeV LEP2 run already places the limit of $\Lambda \gtrsim 0.7$ (1.4) TeV on vector-like (tensor-like) four-Fermi effective operators. Similarly, the future 200 GeV LEP2 run can place a limit of $\Lambda \gtrsim 1.5$ (2.5) TeV and, at a 1000 GeV NLC, the corresponding limits are remarkably strong: $\Lambda \gtrsim 17$ (27) TeV; better (due to a negligible SM background) than those obtainable for flavor diagonal four-Fermi operators, such as $ttee$.

Finally, concerning the limits on the scale of the effective operators that give rise to new htc scalar interaction, we found, for example, that $\Lambda \gtrsim 830$ GeV at a 500 GeV NLC via the Bjorken process, and $\Lambda \gtrsim 2150$ GeV at a 1.5 TeV NLC via the WW -fusion process, if the mass of the SM Higgs boson is ~ 250 GeV.

ACKNOWLEDGMENTS

We thank D. Atwood, G. Eilam and A. Soni for discussions. This research was supported in part by US DOE contract number DE-FG03-94ER40837(UCR).

¹⁰We thank David Atwood for his helpful remarks regarding this point.

-
- [1] For recent reviews on linear colliders see: ECFA/DESY LC Physics Working Group, E. Accomando *et al.*, Phys. Rep. **299**, 1 (1998); NLC ZDR Design Group and NLC Physics Working Group, S. Kuhlman *et al.*, hep-ex/9605011; H. Murayama and M. E. Peskin, Annu. Rev. Nucl. Part. Sci. **49**, 513 (1996).
- [2] G. Eilam, J.L. Hewett and A. Soni, Phys. Rev. D **44**, 1473 (1991); **59**, 039901(E) (1998).
- [3] W. Buchmüller and M. Gronau, Phys. Lett. B **220**, 641 (1989); H. Fritzsch, *ibid.* **224**, 423 (1989); J.L. Diaz-Cruz, R. Martinez, M.A. Perez and A. Rosado, Phys. Rev. D **41**, 891 (1990); B. Dutta-Roy *et al.*, Phys. Rev. Lett. **65**, 827 (1990); J.L. Diaz-Cruz and G. Lopez Castro, Phys. Lett. B **301**, 405 (1993); B. Mele, S. Petrarca and A. Soddu, *ibid.* **435**, 401 (1998).
- [4] A. Axelrod, Nucl. Phys. **B209**, 349 (1982); M. Clements *et al.*, Phys. Rev. D **27**, 570 (1983); V. Ganapathi *et al.*, *ibid.* **27**, 579 (1983); G. Eilam, *ibid.* **28**, 1202 (1983); C.-H. Chang *et al.*, Phys. Lett. B **313**, 389 (1993); C.-S. Huang, X.-H. Wu and S.-H. Zhu, *ibid.* **452**, 143 (1999).
- [5] W.-S. Hou, Phys. Lett. B **296**, 179 (1992); M. Luke and M.J. Savage, *ibid.* **307**, 387 (1993); J.L. Diaz-Cruz *et al.*, hep-ph/9903299.
- [6] D. Atwood, L. Reina, and A. Soni, Phys. Rev. D **55**, 3156 (1997).
- [7] S. Bar-Shalom, G. Eilam, A. Soni, and J. Wudka, Phys. Rev. Lett. **79**, 1217 (1997); Phys. Rev. D **57**, 2957 (1998).
- [8] M.J. Duncan, C.S. Li, R.J. Oakes, and J.M. Yang, Phys. Rev. D **31**, 1139 (1985); **49**, 293 (1994); **56**, 3156(E) (1997); J.-M. Yang and C.-S. Li, *ibid.* **49**, 3412 (1994); **51**, 3974(E) (1995); G. Couture, C. Hamzaoui, and H. König, *ibid.* **52**, 1713

- (1995); J.L. Lopez, D.V. Nanopoulos, and R. Rangarajan, *ibid.* **56**, 3100 (1997); G. Couture, M. Frank, and H. König, *ibid.* **56**, 4213 (1997); G.M. de Divitiis, R. Petronzio, and L. Silvestrini, Nucl. Phys. **B504**, 45 (1997).
- [9] J.M. Yang, B.-L. Young, and X. Zhang, Phys. Rev. D **58**, 055001 (1998).
- [10] S. Bar-Shalom, G. Eilam and A. Soni, Phys. Rev. D **60**, 035007 (1999).
- [11] D. Atwood, L. Reina and A. Soni, Phys. Rev. Lett. **75**, 3800 (1995); Phys. Rev. D **53**, 1199 (1996); W.-S. Hou and G.-L. Lin, Phys. Lett. B **379**, 261 (1996); J. Yi *et al.*, Phys. Rev. D **57**, 4343 (1998); W.-S. Hou, G.-L. Lin, and C.-Y. Ma, *ibid.* **56**, 7434 (1997); M. Sher, hep-ph/9809590.
- [12] Z.-H. Yu *et al.* hep-ph/9903471; M. Chemtob and G. Moreau, Phys. Rev. D **59**, 116012 (1999); U. Mahanta and A. Ghosal, *ibid.* **57**, 1735 (1998).
- [13] F. del Aguila, J. A. Aguilar-Saavedra, and R. Miquel, Phys. Rev. Lett. **82**, 1628 (1999).
- [14] W. Buchmuller and D. Wyler, Nucl. Phys. **B268**, 621 (1986); C. Arzt, M.B. Einhorn, and J. Wudka, Nucl. Phys. **B433**, 41 (1995).
- [15] S. Bar-Shalom and J. Wudka, hep-ph/9904365.
- [16] K. Hikasa, Phys. Lett. **149B**, 221 (1984).
- [17] T. Han and J.L. Hewett, Phys. Rev. D **60**, 074015 (1999).
- [18] V.F. Obraztsov, S.R. Slabospitsky, and O.P. Yushchenko, Phys. Lett. B **426**, 393 (1998).
- [19] D. Atwood and M. Sher, Phys. Lett. B **411**, 221 (1997).
- [20] K.J. Abraham, K. Whisnant, and B.-L. Young, Phys. Lett. B **419**, 381 (1998).
- [21] A. Djouadi *et al.*, in *Physics and Experiments with Linear Colliders*, edited by R. Orava *et al.*, Saariseka, Finland, 1991 [Int. J. Mod. Phys. A (Proc. Suppl.) **1A&B** (1993)].
- [22] B. Grzadkowski, Acta Phys. Pol. B **27**, 921 (1996); B. Grzadkowski, Z. Hioki, and M. Szafranski, Phys. Rev. D **58**, 035002 (1998).
- [23] A. Manohar and H. Georgi, Nucl. Phys. **B234**, 189 (1984).
- [24] S. Dawson, Nucl. Phys. **B249**, 42 (1985); S. Dawson and S. S. D. Willenbrock, *ibid.* **B284**, 449 (1987); P.W. Johnson, F.I. Olness and W.-K. Tung, Phys. Rev. D **36**, 291 (1987); R.P. Kauffman, *ibid.* **41**, 3343 (1990).
- [25] See e.g., V. Barger and R. Phillips, *Collider Physics* (Addison-Wesley, Redwood City, CA, 1987).
- [26] See e.g., R. Frey, in *Proceedings of the Workshop on Physics and Experiments with Linear Colliders*, edited by A. Miyamoto, Y. Fujii, T. Matsui, and S. Iwata (World Scientific, Singapore, 1996), hep-ph/9606201.
- [27] B. Shen (private communication).
- [28] C.R. Schmidt and M. Peskin, Phys. Rev. Lett. **69**, 410 (1992).
- [29] B. Grzadkowski and J.F. Gunion, Phys. Lett. B **350**, 218 (1995).
- [30] Particle Data Group, C. Caso *et al.*, Eur. Phys. J. C **3**, 1 (1998).
- [31] See e.g., J.F. Gunion, H.E. Haber, G. Kane, and S. Dawson, *The Higgs Hunter's Guide* (Addison-Wesley, Redwood City, CA, 1990).
- [32] For examples of other types of t -channel singularities see R.F. Piers, Phys. Rev. Lett. **6**, 641 (1961); I.F. Ginzburg, hep-ph/9509314; K. Melnikov and V.G. Serbo, Nucl. Phys. **B483**, 67 (1997).
- [33] T. Han, R.D. Peccei and X. Zhang, Nucl. Phys. **B454**, 527 (1995).
- [34] F. del Aguila, J. A. Aguilar-Saavedra, and Ll. Ametller, hep-ph/9906462.